
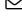






Prompt-based Tuning of Transformer Models for Multi-Center Medical Image Segmentation

Numan Saeed  , Muhammad Ridzuan , Roba Al Majzoub , and
Mohammad Yaqub  

Mohamed bin Zayed University of Artificial Intelligence, Abu Dhabi, UAE
{numan.saeed, muhammad.ridzuan, roba.majzoub,
mohammad.yaqub}@mbzuai.ac.ae

Abstract. Medical image segmentation is a vital healthcare endeavor requiring precise and efficient models for appropriate diagnosis and treatment. Vision transformer-based segmentation models have shown great performance in accomplishing this task. However, to build a powerful backbone, the self-attention block of ViT requires large-scale pre-training data. The present method of modifying pre-trained models entails updating all or some of the backbone parameters. This paper proposes a novel fine-tuning strategy for adapting a pretrained transformer-based segmentation model on data from a new medical center. This method introduces a small number of learnable parameters, termed prompts, into the input space (less than 1% of model parameters) while keeping the rest of the model parameters frozen. Extensive studies employing data from new unseen medical centers show that prompts-based fine-tuning of medical segmentation models provides excellent performance on the new center data with a negligible drop on the old centers. Additionally, our strategy delivers great accuracy with minimum re-training on new center data, significantly decreasing the computational and time costs of fine-tuning pre-trained models. Our source code will be publicly available.

Keywords: Transfer Learning · Vision Transformer · Medical Image Segmentation · Limited Data · Prompt-based Tuning.

1 Introduction

Recently, several novel segmentation models have been proposed to assist in medical image analysis and understanding, leading to faster and more accurate treatment planning [1,14,18]. Many of these proposed models are increasingly transformer-based, demonstrating excellent performance on several medical datasets. Transformers are a class of neural network topologies distinguished chiefly by their heavy usage of the attention mechanism [15]. In particular, Vision Transformers (ViTs) [6] have demonstrated their ability in 3D medical image segmentation. However, ViTs exhibit an intrinsic lack of image-specific inductive bias and scaling behavior; nonetheless, this lack is mitigated by utilizing large datasets and large model capacity.

On the other hand, medical datasets are limited in size due to time-consuming and expensive expert annotations, which hinders the use of powerful transformer models to their full capacity. A common approach to handle the limited data size in the medical domain is to use transfer learning [17]. This technique aims to reuse model weights or parameters of already trained ViTs on different but related tasks. More specifically, models are first pretrained on a different large dataset; the weights of the pretrained model act as informed initializations of the model [4,5,11]. The pretrained model is then fine-tuned on the target dataset, yielding faster training and a more generalizable model.

However, the limited size of medical datasets is not the only challenge; medical datasets are sourced from different medical centers that use different machines and acquisition protocols, leading to further heterogeneity in the acquired data [7,12]. As a result, a model trained on data obtained from specific medical centers might fail to perform well on data obtained from a new medical center. Conventionally, we can use the transfer learning technique for adapting the pretrained model to the new medical center data. One such effective adaptation strategy is full fine-tuning, in which all the parameters of the pretrained model will be fine-tuned on the new center’s data. However, directly fine-tuning a pre-trained transformer model on a new center’s data can lead to overfitting (as we have mostly small-size datasets from any new center) and loss of knowledge learned from the previous centers [2,10]. Hence, this strategy requires storing and deploying a separate copy of the backbone parameters for every newly acquired medical center data. This strategy is, however, costly and infeasible if the end solution is regularly deployed on new medical centers or the acquisition protocol and/or machines in an existing center change. Particularly, this infeasibility will be more prominent in transformer-based models, as they are significantly larger than their convolutional neural network (CNN) counterparts.

In this work, we propose a prompt-based fine-tuning method of ViTs on new medical centers’ data. Instead of altering or fine-tuning the pretrained Transformer, we introduce center-specific learnable token parameters called prompts in the input space of the segmentation model. Only prompts and the output convolutional layer are learnable during the fine-tuning of the model on the new center’s data. The rest of the entire pre-trained-Transformer model is frozen. We show that this method can achieve high accuracies on new centers’ data with a negligible loss on the accuracy of the old centers, in contrast to full or partial fine-tuning techniques, where the model accuracy decreases on the old center data. The main contributions of this work are:

- We propose a new *Prompt*-based fine-tuning technique for the *Transformer* based medical image segmentation models, which reduces the fine-tuning time and the number of learnable parameters (less than 1% of the model parameters) to be stored for the new medical center.
- The proposed method achieves equivalent accuracy for new center data compared to the full fine-tuning technique while mostly preserving the accuracy for old center data that is compromised in full-fine-tuning.

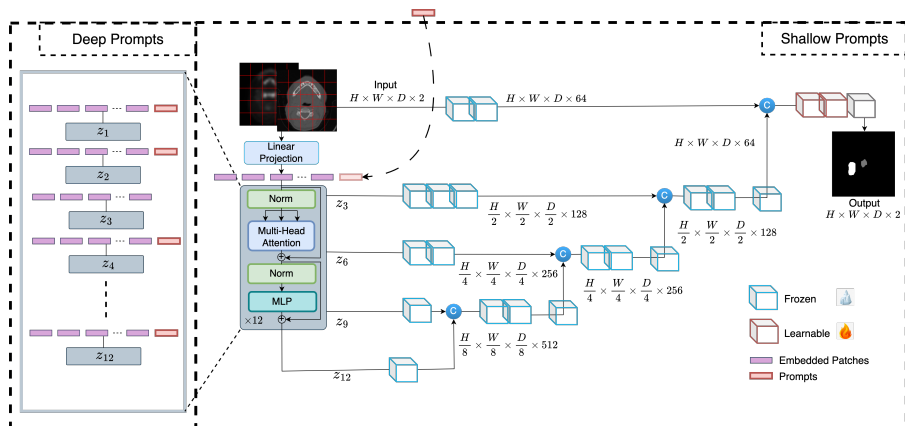


Fig. 1: Overview of the proposed method. Learnable prompts are appended to the embedded tokens in the input space and passed through the Transformer encoder but not the decoder during the fine-tuning. In Deep prompt-based fine-tuning, the learnable prompts are replaced by new prompts after each transformer layer.

- We showcase the efficacy of the proposed method on *multi-class* segmentation of head and neck cancer tumors using *multi-channel* computed tomography (CT) and positron emission tomography (PET) scans of patients obtained from *multi-center* (seven centers) sources.

2 Methodology

In this section, we describe the prompt-based tuning for adapting transformer-based medical image segmentation models. Prompt-based fine-tuning technique injects a small number of learnable parameters into the Transformer’s input space and keeps the backbone frozen during the downstream training stage. The overall framework is presented in Figure 1. We demonstrate two variants of prompt-based tuning, shallow and deep, and compare their performance to the conventional fine-tuning methods such as partial and full fine-tuning. Below, we describe the two prompt-based tuning methods and highlight the differences between the two.

Shallow prompt tuning: In shallow prompt fine-tuning, a set of p continuous prompts of dimension d are introduced in the input space after the embedding layer. These prompts are concatenated with the token embeddings of the volumetric patches of an input image $x \in \mathbb{R}^{H \times W \times D \times C}$, where H , W , D , and C are the height, width, depth, and channels of the 3D image, respectively. $K \times K \times K$ represents the dimensions of each patch, and $n = HWD/K^3$ is the number of patches extracted. The embedding layer projects these patches to a dimension

d. The class token is dropped from the ViT [6] as the experiments are for a segmentation task. The resulting concatenated prompts and embeddings are fed to a transformer encoder consisting of L layers, following the same pipeline as the original ViT [6], with normalization, multi-head self-attention (MSA), and multi-layer perceptron. The decoder only uses image patch embeddings as inputs, and prompt embeddings are discarded. The shallow prompt-based fine-tuning is formulated as:

$$x_0 = \text{Embedding}(x) \quad x_0 \in \mathbb{R}^{n \times d} \quad (1)$$

$$[Z_1, x_1] = \text{Encoder}_1([P, x_0]) \quad P \in \mathbb{R}^{p \times d} \quad (2)$$

$$[Z_i, x_i] = \text{Encoder}_i([Z_{i-1}, x_{i-1}]) \quad i = 2, \dots, L \quad (3)$$

$$Y_{seg} = \text{Decoder}(\text{ConvTrans3D}(x_i)) \quad i = 3, 6, 9, 12 \quad (4)$$

where P is the prompt matrix and *ConvTrans3D* refers to 3D transpose convolution.

Deep prompt tuning In deep prompt fine-tuning, the prompts can be introduced at the input space of each transformer layer or subset of layers. In our implementation, we add the deep prompts after each skip connection layer:

$$[-, x_i] = \text{Encoder}_i([P_{i-1}, x_{i-1}]) \quad i = 1, \dots, L \quad (5)$$

3 Experiments

We study two transformer-based 3D segmentation architectures, UNETR [8] and Swin-UNETR [9]. In addition, we compare the proposed method to partial and full fine-tuning, two prevalent transfer learning protocols used in medical imaging.

3.1 Dataset

The dataset used in this work is multi-center, multi-class, and multi-modal. This dataset is comprised of head and neck cancer patient scans collected from seven centers. The data consists of CT and PET scans, as well as electronic health records (EHR) of each patient. The PET volume is registered with the CT volume to a common origin, although they each have varying sizes and resolutions. The CT sizes range from (128, 128, 67) to (512, 512, 736), while the PET sizes range from (128, 128, 66) to (256, 256, 543) voxels. The CT resolutions range from (0.488, 0.488, 1.00) to (2.73, 2.73, 2.80), while the PET resolutions range from (2.73, 2.73, 2.00) to (5.47, 5.47, 5.00) mm in the x , y , and z directions.

The dataset contains segmentation masks for each patient, including the ground truth of primary Gross Tumor Volumes (GTVp), nodal Gross Tumor Volumes (GTVn), and other clinical information. The annotations were made

by medical professionals at the respective centers and are provided with the dataset. The dataset is publicly available on the MICCAI 2022 HEad and neCK TumOR (HECKTOR) challenge website [13]. The complete dataset consists of 524 samples. The detailed distribution of the dataset across different centers is listed in Table 1 along with the type of machines used to acquire the scans.

3.2 Experimental Setup

The dataset for each of the seven centers is first split into train and test sets for a fair comparison. In all experiments, the model is first pre-trained using the six centers’ training data and then fine-tuned on the seventh center’s training data. We evaluate the performance of the model on 1) the seventh center’s test set (new center) and 2) on the six centers’ test set (old centers). We compare both metrics for the following fine-tuning techniques as shown in Fig. 3.

No Fine-tuning: In this, the pre-trained model is directly used to infer the test samples without any fine-tuning.

Partial Fine-tuning: This technique involves fine-tuning the pre-trained model’s last decoder block using the seventh center’s training set.

Full Fine-tuning: This technique involves fine-tuning the entire pre-trained model using the seventh center’s training set.

Shallow Prompt Fine-tuning: This is a variant of prompt-based fine-tuning, where the prompts are introduced only in the input space. Only the prompts and the final convolutional layer are trainable during fine-tuning, while the rest of the model is frozen.

Deep Prompt Fine-tuning: This technique is similar to shallow prompt fine-tuning; prompts at each level of the transformer layer are introduced. Thus, at each level, there are new trainable prompts to refine.

3.3 Implementation Details

We implement all our models using the PyTorch framework and train them on a single NVIDIA Tesla A6000 GPU. The details of the experimental settings for all fine-tuning techniques are listed in Supplementary Table 5. We also list the pre-processing and augmentation details of the data in Supplementary Table 6.

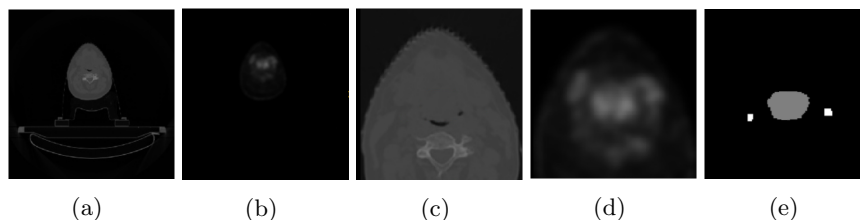


Fig. 2: A sample of images from the dataset. (a) and (b) depict the original CT and PET scans, respectively. (c) and (d) show the cropped CT and PET scans, and (e) shows the cropped ground truth mask.

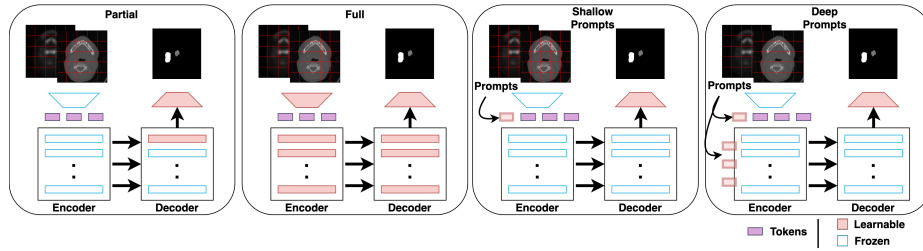


Fig. 3: Illustrations of the different fine-tuning methods including partial and full fine-tuning (conventional) as well as shallow and deep prompt-based (proposed).

3.4 Results

Table 2 presents the results of fine-tuning the pre-trained UNETR and Swin-UNETR on the old and new medical center datasets. We conduct our evaluations using a 5-fold cross-validation for a total of 290 experiments. The results of all the folds for all the centers can be found in the supplementary material. We use Dice score [3] to evaluate the performance of segmentation in our experiments. We can observe that:

Table 1: Dataset origin and distribution.

Center	Country	PET/CT scanner	#Samples
HGJ	Canada	Discovery ST, GE Healthcare	55
CHUS	Canada	GeminiGXL 16, Philips	72
HMR	Canada	Discovery STE, GE Healthcare	18
CHUM	Canada	Discovery STE, GE Healthcare	56
CHUV	Switzerland	Discovery D690 TOF, GE Healthcare	53
CHUP	France	Biograph mCT 40 ToF, Siemens	72
MDA	USA	Discovery HR, RX, ST, STE (GE Healthcare)	197

Table 2: Aggregated Dice score of GTVp and GTVn using different fine-tuning techniques with UNETR and Swin-UNETR.

Model	Fine-tuning	None		Partial		Full		Shallow Prompts		Deep Prompts	
		Old	New	Old	New	Old	New	Old	New	Old	New
UNETR	Center(s)	0.7869	0.6708	0.7027	0.7153	0.7048	0.7298	0.7507	0.7136	0.7644	0.7198
	CHUP	0.7665	0.7699	0.7574	0.7852	0.7574	0.7855	0.7683	0.7807	0.7688	0.7831
	CHUS	0.7674	0.7877	0.7479	0.7949	0.7439	0.7981	0.7607	0.7938	0.7639	0.7913
	HGJ	0.7659	0.7224	0.7635	0.7298	0.7609	0.7533	0.7667	0.7339	0.7657	0.7379
	MDA	0.7704	0.7321	0.7622	0.7459	0.7665	0.7539	0.7723	0.7501	0.7724	0.7531
	CHUV	0.7765	0.7714	0.7584	0.7721	0.7623	0.7759	0.7734	0.7775	0.7753	0.7799
	CHUM	0.7731	0.6712	0.7629	0.6987	0.7726	0.7099	0.7769	0.6992	0.7760	0.7080
Swin-UNETR	CHUP	0.7584	0.7695	0.7569	0.7890	0.7541	0.7905	0.7613	0.7797	-	-
	CHUS	0.7763	0.7684	0.7642	0.7685	0.7667	0.7706	0.7719	0.7698	-	-
	CHUM	0.7835	0.6609	0.6960	0.7373	0.7026	0.7419	0.7320	0.7136	-	-
	MDA	0.7616	0.7291	0.7644	0.7413	0.7541	0.7522	0.7590	0.7352	-	-

Table 3: Total number of learnable parameters for different fine-tuning techniques.

Model	Fine-tuning	None	Partial	Full	Shallow Prompts	Deep Prompts
UNETR	-	0.025M	96M	0.038M	0.15M	
Swin-UNETR	-	0.055M	62M	0.073M		-

1. All the different fine-tuning techniques yield better performance for the new centers than direct inference on the pre-trained models.
2. Shallow prompt-based fine-tuning achieves higher, or comparable Dice score on the new center data, with nearly the same number of learnable parameters as partial fine-tuning (see Table 3). However, shallow prompts outperform partial and full fine-tuning techniques for all seven centers on the old centers’ data.
3. Deep prompt-based fine-tuning achieves the same Dice score as full fine-tuning on the new center data but with significantly fewer learnable parameters. In addition, deep prompt-based fine-tuning outperforms the full fine-tuning on old centers’ data for all seven centers. Thus, even if the storage of model weights is not a concern, prompt-based fine-tuning is still a promising approach for fine-tuning models as it retains more knowledge related to old centers.
4. Prompt-based fine-tuning of Swin-UNETR exhibits a similar pattern to that of UNETR. However, the loss in performance on old center data for the conventional fine-tuning methods is less prominent for some centers compared to that of UNETR. This can be explained by the inductive biases in Swin-UNETR, which employs MSA within local shifted windows and merges patch embeddings at deeper layers. Swin-UNETR requires further optimization with regard to prompt position to improve its performance further.

4 Discussion

This work introduces a new method for fine-tuning transformer-based medical segmentation models on new center data. Our method is more efficient than conventional approaches, requiring fewer parameters at a less computational cost while achieving the same or better performance on new center data when compared to conventional methods. We show superior performance for prompt-based fine-tuning compared to other techniques, achieving a statistically significant increase in the Dice score for old centers. We note the difference in performance between CHUP and CHUS, which have similar number of samples but different acquisition machines and origins. CHUP exhibits a larger drop in performance on the old centers than CHUS (nearly 8% in CHUP vs. 1% in CHUS for partial and full fine-tuning). This is likely due to the larger dataset distribution shift in

Table 4: Non-parametric paired one-tailed t-test (Wilcoxon signed-rank test) on whether deep prompt-based fine-tuning of UNETR performance is better than the other methods (p -value < 0.05).

	Partial?	Full?	Shallow?
Is the performance of deep-prompt based fine-tuned models on old centers statistically better than	✓	✓	×
Is the performance of deep-prompt based fine-tuned models on new centers statistically better than	✓	×	✓

CHUP compared to the rest of the centers. However, if shallow- or deep-prompt-based fine-tuning is used, the drop is only 2-3%. We perform a non-parametric paired one-tailed t-test (Wilcoxon signed-rank test [16]) to assess whether deep prompt-based tuning of medical segmentation models is significantly better than other fine-tuning techniques on old and new centers’ data (the null hypothesis H_0 states that the segmentation performance of deep-prompt based fine-tuning is statistically the same as the other techniques. The alternative hypothesis H_1 states that the deep-prompt-based technique outperforms the other methods). Table 4 presents the results of each test; it can be observed that deep prompt-based fine-tuning outperforms full and partial fine-tuning techniques on the old center’s data. Similarly, it outperforms the partial and shallow prompt-based techniques on the new center data. However, the test fails on the new center’s data for full-fine tuning. Thus, we proceed to perform a two-tailed t-test and confirm that the performance of deep prompt-based fine-tuning and full fine-tuning on new center data are statistically the same (p -value < 0.05).

In our experiments, we observed that the extra learnable prompts at deeper layers in the deep prompt-based fine-tuning improve the performance compared to shallow prompt-based fine-tuning, which only inserts prompts in the input space after the patch embedding layer. Furthermore, we found in the ablation studies that adding learnable prompts before the first layer of the transformer and after each skip connection layer of the encoder gives almost the same accuracy as adding the learnable prompts at each transformer layer. This suggests that adding too many prompts in the deeper layers can over-parameterize the model, which may result in overfitting on new center data. Further studies will be conducted to quantify the effect of the number and position of the prompts.

5 Conclusion

We propose a prompt-based fine-tuning framework for the medical image segmentation problem. This method takes advantage of the strength of transformers to handle a variable number of tokens at the input and the deeper layers. We validate our proposed method by training transformer-based segmentation models on head and neck PET/CT scans and compare our results with conventional fine-tuning techniques. Although we were able to show the efficacy of the proposed method on medical image segmentation problems, further investigation is

needed to study its scalability to other transformer-based segmentation models in the future. In addition, investigation of prompt-based learning in different tasks such as classification and prognosis is needed to assess its efficacy.

References

1. Alalwan, N., Abozeid, A., ElHabshy, A., Alzahrani, A.: Efficient 3d deep learning model for medical image semantic segmentation. *Alexandria Engineering Journal* **60**(1), 1231–1239 (2021). <https://doi.org/https://doi.org/10.1016/j.aej.2020.10.046>, <https://www.sciencedirect.com/science/article/pii/S1110016820305639>
2. Barone, A.V.M., Haddow, B., Germann, U., Sennrich, R.: Regularization techniques for fine-tuning in neural machine translation. *CoRR* **abs/1707.09920** (2017), <http://arxiv.org/abs/1707.09920>
3. Bertels, J., Eelbode, T., Berman, M., Vandermeulen, D., Maes, F., Bisschops, R., Blaschko, M.B.: Optimizing the dice score and jaccard index for medical image segmentation: Theory & practice. vol. *abs/1911.01685* (2019), <http://arxiv.org/abs/1911.01685>
4. Chen, T., Kornblith, S., Norouzi, M., Hinton, G.E.: A simple framework for contrastive learning of visual representations. *CoRR* **abs/2002.05709** (2020), <https://arxiv.org/abs/2002.05709>
5. Chen, X., Fan, H., Girshick, R.B., He, K.: Improved baselines with momentum contrastive learning. *CoRR* **abs/2003.04297** (2020), <https://arxiv.org/abs/2003.04297>
6. Dosovitskiy, A., Beyer, L., Kolesnikov, A., Weissenborn, D., Zhai, X., Unterthiner, T., Dehghani, M., Minderer, M., Heigold, G., Gelly, S., Uszkoreit, J., Houlsby, N.: An image is worth 16x16 words: Transformers for image recognition at scale. *CoRR* **abs/2010.11929** (2020), <https://arxiv.org/abs/2010.11929>
7. Glocker, B., Robinson, R., Castro, D.C., Dou, Q., Konukoglu, E.: Machine learning with multi-site imaging data: An empirical study on the impact of scanner effects (2019). <https://doi.org/10.48550/ARXIV.1910.04597>, <https://arxiv.org/abs/1910.04597>
8. Hatamizadeh, A., Tang, Y., Nath, V., Yang, D., Myronenko, A., Landman, B., Roth, H.R., Xu, D.: Unetr: Transformers for 3d medical image segmentation. In: *2022 IEEE/CVF Winter Conference on Applications of Computer Vision (WACV)*. pp. 1748–1758. IEEE Computer Society, Los Alamitos, CA, USA (jan 2022). <https://doi.org/10.1109/WACV51458.2022.00181>, <https://doi.ieeecomputersociety.org/10.1109/WACV51458.2022.00181>
9. Hatamizadeh, A., Nath, V., Tang, Y., Yang, D., Roth, H.R., Xu, D.: Swin unetr: Swin transformers for semantic segmentation of brain tumors in mri images. In: Crimi, A., Bakas, S. (eds.) *Brainlesion: Glioma, Multiple Sclerosis, Stroke and Traumatic Brain Injuries*. pp. 272–284. Springer International Publishing, Cham (2022)
10. Kumar, A., Raghunathan, A., Jones, R., Ma, T., Liang, P.: Fine-tuning can distort pretrained features and underperform out-of-distribution (2022). <https://doi.org/10.48550/ARXIV.2202.10054>, <https://arxiv.org/abs/2202.10054>
11. Lin, K., Heckel, R.: Vision transformers enable fast and robust accelerated MRI. In: Konukoglu, E., Menze, B., Venkataraman, A., Baumgartner, C., Dou, Q., Albarqouni, S. (eds.) *Proceedings of The 5th International Conference on Medical*

- Imaging with Deep Learning. *Proceedings of Machine Learning Research*, vol. 172, pp. 774–795. PMLR (06–08 Jul 2022), <https://proceedings.mlr.press/v172/lin22a.html>
12. Ma, Q., Zhang, T., Zanetti, M.V., Shen, H., Satterthwaite, T.D., Wolf, D.H., Gur, R.E., Fan, Y., Hu, D., Busatto, G.F., Davatzikos, C.: Classification of multi-site mr images in the presence of heterogeneity using multi-task learning. *NeuroImage: Clinical* **19**, 476–486 (2018). <https://doi.org/https://doi.org/10.1016/j.nicl.2018.04.037>, <https://www.sciencedirect.com/science/article/pii/S2213158218301463>
 13. Oreiller, V., Andrearczyk, V., Jreige, M., Boughdad, S., Elhalawani, H., Castelli, J., Vallières, M., Zhu, S., Xie, J., Peng, Y., Iantsen, A., Hatt, M., Yuan, Y., Ma, J., Yang, X., Rao, C., Pai, S., Ghimire, K., Feng, X., Naser, M.A., Fuller, C.D., Yousefirizi, F., Rahmim, A., Chen, H., Wang, L., Prior, J.O., Depeursinge, A.: Head and neck tumor segmentation in pet/ct: The hecktor challenge. *Medical Image Analysis* **77**, 102336 (2022). <https://doi.org/https://doi.org/10.1016/j.media.2021.102336>, <https://www.sciencedirect.com/science/article/pii/S1361841521003819>
 14. Valanarasu, J.M.J., Oza, P., Hacihaliloglu, I., Patel, V.M.: Medical transformer: Gated axial-attention for medical image segmentation. In: de Bruijne, M., Cattin, P.C., Cotin, S., Padoy, N., Speidel, S., Zheng, Y., Essert, C. (eds.) *Medical Image Computing and Computer Assisted Intervention – MICCAI 2021*. pp. 36–46. Springer International Publishing, Cham (2021)
 15. Vaswani, A., Shazeer, N., Parmar, N., Uszkoreit, J., Jones, L., Gomez, A.N., Kaiser, L.u., Polosukhin, I.: Attention is all you need **30** (2017), <https://proceedings.neurips.cc/paper/2017/file/3f5ee243547dee91fbd053c1c4a845aa-Paper.pdf>
 16. Wilcoxon, F.: *Individual Comparisons by Ranking Methods*, pp. 196–202. Springer New York, New York, NY (1992)
 17. Yu, X., Wang, J., Hong, Q.Q., Teku, R., Wang, S.H., Zhang, Y.D.: Transfer learning for medical images analyses: A survey. *Neurocomputing* **489**, 230–254 (2022). <https://doi.org/https://doi.org/10.1016/j.neucom.2021.08.159>, <https://www.sciencedirect.com/science/article/pii/S0925231222003174>
 18. Zhou, H., Guo, J., Zhang, Y., Yu, L., Wang, L., Yu, Y.: nnformer: Interleaved transformer for volumetric segmentation. *CoRR* **abs/2109.03201** (2021), <https://arxiv.org/abs/2109.03201>

Table 5: Experimental settings for the different fine-tuning techniques.

Hyperparameters	Full	Shallow Prompt	Deep Prompt
Optimizer	AdamW	SGD	SGD
lr	1e-5	0.05	0.05
Weight decay	1e-3	0	0
Learning rate schedule	-	cosine decay	cosine decay
Total epochs	100	100	100
Batch size	3	3	3

Table 6: Preprocessing and augmentation details.

Augmentations	axis	probability	size
Orientation	PLS	-	-
CT/PET Concatenation	1	-	-
Normalization	-	-	-
Random Crop	-	0.5	96 × 96 × 96
Random flip	x, y, z	0.2	-
Rotate by 90 (up to 3×)	x, y	0.2	-

Table 7: 5-fold results for UNETR on CHUP center

Fold	No Finetuning	Partial Finetuning	Full Finetuning	Shallow Prompt	Deep Prompt
1	0.6112	0.6813	0.6307	0.6312	0.6344
2	0.7442	0.7917	0.7596	0.7519	0.7449
3	0.6399	0.6627	0.7285	0.6910	0.6926
4	0.6919	0.7241	0.7551	0.7417	0.7518
5	0.6663	0.7165	0.7753	0.7523	0.7751
$\mu \pm \sigma$	0.6708±0.0509	0.7153±0.0496	0.7298±0.0579	0.7136±0.0526	0.7198±0.0564

Table 8: 5-fold results for UNETR on CHUS center

Fold	No Finetuning	Partial Finetuning	Full Finetuning	Shallow Prompt	Deep Prompt
1	0.7861	0.8061	0.8058	0.8035	0.8150
2	0.7825	0.7975	0.7884	0.7886	0.7842
3	0.6875	0.6981	0.6906	0.6903	0.6912
4	0.7947	0.8196	0.8125	0.8103	0.8176
5	0.7987	0.8047	0.8300	0.8107	0.8075
$\mu \pm \sigma$	0.7699±0.0465	0.7852±0.0493	0.7855±0.0551	0.7807±0.0513	0.7831±0.053

Table 9: 5-fold results for UNETR on CHUM center

Fold	No Finetuning	Partial Finetuning	Full Finetuning	Shallow Prompt	Deep Prompt
1	0.8009	0.8017	0.8089	0.8086	0.8133
2	0.7387	0.7343	0.7414	0.7410	0.7392
3	0.7626	0.7559	0.7541	0.7702	0.7733
4	0.7668	0.7690	0.7675	0.7697	0.7629
5	0.7882	0.7995	0.8077	0.7981	0.8048
$\mu \pm \sigma$	0.7714 \pm 0.0241	0.7721 \pm 0.0288	0.7759 \pm 0.0309	0.7775 \pm 0.0266	0.7799 \pm 0.0294

Table 10: 5-fold results for UNETR on CHUV center

Fold	No Finetuning	Partial Finetuning	Full Finetuning	Shallow Prompt	Deep Prompt
1	0.6368	0.6496	0.6633	0.6555	0.6454
2	0.7516	0.7631	0.7667	0.7609	0.7682
3	0.7832	0.8014	0.8013	0.8091	0.8063
4	0.8243	0.8340	0.8422	0.8339	0.8413
5	0.6645	0.6812	0.6959	0.6910	0.7043
$\mu \pm \sigma$	0.7321 \pm 0.0793	0.7459 \pm 0.0784	0.7539 \pm 0.0738	0.7501 \pm 0.0759	0.7531 \pm 0.0788

Table 11: 5-fold results for UNETR on MDA center

Fold	No Finetuning	Partial Finetuning	Full Finetuning	Shallow Prompt	Deep Prompt
1	0.7258	0.7284	0.7750	0.7492	0.7571
2	0.7384	0.7457	0.7736	0.7464	0.7538
3	0.6843	0.6970	0.7159	0.6979	0.7000
4	0.7426	0.7500	0.7584	0.7504	0.7515
5	0.7207	0.7279	0.7434	0.7258	0.7271
$\mu \pm \sigma$	0.7224 \pm 0.0231	0.7298 \pm 0.0209	0.7533 \pm 0.0245	0.7339 \pm 0.0225	0.7379 \pm 0.0243

Table 12: 5-fold results for UNETR on HGJ center

Fold	No Finetuning	Partial Finetuning	Full Finetuning	Shallow Prompt	Deep Prompt
1	0.7887	0.8024	0.8062	0.7994	0.7955
2	0.7511	0.7534	0.7622	0.7543	0.7566
3	0.8100	0.8031	0.8075	0.8125	0.8114
4	0.8035	0.8225	0.8262	0.8148	0.8191
5	0.7852	0.7935	0.7883	0.7878	0.7739
$\mu \pm \sigma$	0.7877 \pm 0.0229	0.7949 \pm 0.0255	0.7981 \pm 0.0241	0.7938 \pm 0.0246	0.7913 \pm 0.0259

Table 13: 5-fold results for UNETR on HMR center

Fold	No Finetuning	Partial Finetuning	Full Finetuning	Shallow Prompt	Deep Prompt
1	0.6632	0.6903	0.7132	0.7201	0.7453
2	0.7001	0.7188	0.7265	0.7076	0.7194
3	0.6796	0.6797	0.6933	0.6829	0.6854
4	0.5926	0.6229	0.6400	0.6299	0.6264
5	0.7203	0.7817	0.7762	0.7554	0.7632
$\mu \pm \sigma$	0.6712 \pm 0.0489	0.6987 \pm 0.058	0.7098 \pm 0.0496	0.6992 \pm 0.0467	0.708 \pm 0.0542